Research Article

Kai Yu, Yao Wang, Yanxin Li, Jakov Baleta, Jin Wang*, and Bengt Sundén

Effect of phase change materials on heat dissipation of a multiple heat source system

https://doi.org/10.1515/phys-2019-0083
Received Sep 27, 2019; accepted Oct 24, 2019

Abstract: This paper experimentally investigates heat dissipation of a heat pipe with phase change materials (PCMs) cooling in a multiple heat source system. Two heat sources are fixed at one end of the heat pipe. Considering that a heat sink cannot dissipate all the heat generated by two heat sources, various PCMs are used due to a large latent heat. Different materials in a container are wrapped outside of the middle heat pipe to take away the heat from the evaporation section. The experimental tests obtain temperature data of heat source, evaporation section, and energy storage characteristics of PCMs are also determined under constant and dynamic values of the heat source powers. It is found that under this multiple heat source system structure, the phase change material RT35 maintains temperature variations of the evaporation section at a lower temperature and shortens the required time to reach the equilibrium temperature under a heating power of 20 W.

Keywords: phase change material, heat pipe, multiple heat source, electronic cooling, thermal storage

PACS: 44.10.+i, 64.70.D-

1 Introduction

Low heat dissipation efficiency and long reaction time can be easily found in the conventional cooling method for a multiple heat source system. Considerable amounts of heat and many fluctuations are generated in multiple heat source systems, such as multi-core CPUs and highly integrated electronic equipment. Generally, an increase of dissipate heat under a transient high-power operation of a heat source is fulfilled by increasing the power of the cooling fan. Most heat is dissipated by using forced air convection with and without a heat pipe in a periodic or a transient manner. As a latent heat storage material, PCMs (phase change materials) have been widely used in many fields, such as solar thermal energy storage, solar water heating systems, photovoltaic panels, battery thermal management, and electronic devices [1]. An increase in power consumption of electronic devices will result in a temperature rise above a critical value. The latent heat of PCMs can effectively store the instantaneous heat and periodic heat generated by electronic devices, which can prevent the electronic devices from accumulating a large amount of heat in a short time [2]. Al-Jethelah *et al.* [3] numerically studied melting process of PCMs in a latent heat storage system. Nusselt number and melt fraction of PCMs were analyzed to obtain effects of ambient temperature on convective heat transfer coefficient and melting rate. Ebadi *et al.* [4] analyzed performance of the RT35 in a vertical cylindrical thermal energy storage system experimentally and numerically. The results showed that as the melting process progressed, the dominant heat transfer method of RT-35 changed from heat conduction to convective heat transfer. Zhao and Tan [5] presented an evaluation of a prototype thermoelectric system integrated with PCMs for space cooling. Emam *et al.* [6] investigated the passive thermal management of electronic devices and concentrator photovoltaic (CPV) systems with using phase change material, and they found that formation of air cavities inside solid PCMs showed little impact on their cooling performance. Kalbasi *et al.* [7] presented a correlation to estimate the optimum number of fins and optimum volume fraction of PCMs in a heat sink. Mashaei *et al.* [8] pointed out that the heat dissipation in systems with multiple heat sources is not different from that for a single heat source.

Heat pipes integrated with heat sinks have been extensively investigated by using various PCMs [9]. The PCMs show an important role in absorbing dissipated heat of thermal management systems. In 2003, Tan and Tso [10] conducted an experimental study to cool a mobile elec-

***Corresponding Author: Jin Wang:** School of Energy and Environmental Engineering, Hebei University of Technology, Tianjin 300401, China; Email: wjwcn00@163.com
Kai Yu, Yao Wang, Yanxin Li: School of Energy and Environmental Engineering, Hebei University of Technology, Tianjin 300401, China
Jakov Baleta: Faculty of Metallurgy, University of Zagreb, Sisak, Croatia
Bengt Sundén: Department of Energy Sciences, Division of Heat Transfer, Lund University, P.O. Box 118, SE-22100 Lund, Sweden

tronic device using a thermal energy storage unit filled with phase change materials. They found that the temperature distribution was significantly affected by the orientation of the heat storage unit. Wang and Yang [11] numerically investigated variations of operation temperature and melting time by using a PCM based multi-fin heat sink. Results showed that prediction accuracy of transient surface temperature was within 10.2%. In addition, researchers have tried a variety of ways to improve thermal conductivity of PCMs. Wang *et al.* [12] embedded phase change material paraffin into copper foam metal, and results showed that 40% reduction of heat storage time of paraffin wax was obtained by using copper foam. Ebrahimi *et al.* [13] investigated phase change materials in a shell-tube heat exchanger enhanced with heat pipe, and they found that the melting time decreased by 91% compared with no heat pipe case. Abujas *et al.* [14] numerically studied effects of finned pipes and conductive foams on the charge time and the energy distribution. It was found that aluminum fins had a significant reduction on the charge time of the system. In addition, researchers used nanoparticles to increase heat transfer properties of solid and liquid materials. Wang *et al.* [15] experimentally analyzed an effect of different magnetic fields on heat transfer performance of the ferrofluid. It was found that the configuration of adjacent magnetic cannulas could provide a continuous enhancement of convective heat transfer. Chen *et al.* [16] investigated the effect of Fe_3O_4-EGW (a mixture of ethylene glycol and DI-water) nanofluids on heat transfer characteristics in an electric heater. The results show that when 0.5% Fe_3O_4-EGW nanofluid was used, the equilibrium temperature of the middle fin of the electric heater obtained 14.68% enhancement by adding an external magnetic field of 100 mT.

However, most researchers focused on thermal performances of heat sinks and heat pipes under multiple heat sources. Han *et al.* [17] studied a novel flat heat pipe with multiple heat sources, and results showed that both thermal resistance and the maximum heat transport capacity increased with the increase of the number of heat sources. Zhang *et al.* [18] proposed a novel ultra-thin aluminum flat heat pipe to improve thermal performance of two phase device. Results showed that the wicked heat pipes provided an enhancement of thermal performance under inclination angles of 30° and 60°. Chougule and Sahu [19] reported thermal performance of a nanofluid inside a heat pipe with PCMs for electronic cooling. They found that the heat pipe with paraffin reduced the fan power consumption up to 66%, compared with a heat pipe with water as energy storage material. Shabgard and Faghri [20] presented a model of cylindrical heat pipes with multiple heat sources. They focused on the analysis of the constant heat flow and convection cooling during the condensation process, and results from a developed simple method showed good agreement with the full simulation results. Tang *et al.* [21] proposed a cooling method for a multiple heat source heat pipe. Compared with other cooling methods, this multiple heat source and double-end cooling (MSDC) improved the thermal performance of heat pipes.

Based on tests of the charge, discharge and simultaneous charge/discharge performances, Weng *et al.* [22] investigated the thermal performance of a heat pipe with phase change materials. They found that a cooling module with tricosane as PCM saved 46% fan power consumption, compared with the traditional heat pipe. Zhuang *et al.* [23] proposed a novel heat pipe wrapped with PCMs, and they found that the novel composite heat pipe (CHP) filled with 75% PCMs showed a stable temperature reduction of 9.31%, compared to that without PCMs. Behi *et al.* [24] both experimentally and numerically investigated heat dissipation and cooling process of a horizontal PCM-assisted heat pipe. They found that the PCM-assisted heat pipe provided up to 86.7% cooling load under a power range of 50–80 W.

This paper aims to investigate heat dissipation performance of a multiple heat source system under constant and dynamic powers of the heat sources. Various PCMs are used to remove thermal energy from a heat pipe. Thermal performance of the heat pipe with PCMs (deionized water, paraffins RT30, RT35 and RT45) during the charge and discharge processes are tested under different powers of the heat sources. Temperature values on the evaporation section of the heat pipe are discussed to find the optimum PCM for the system heat dissipation.

2 Experimental investigations

2.1 Experimental setup and details

This experimental research aims to investigate cooling performance of PCMs outside a heat pipe with multiple heat sources. Thermocouples are used to measure temperature variations of the heat sources, heat pipe and PCMs. The experimental system consists of a flat heat pipe, two resistors, a container, a fan, heat sinks, two DC power supplies, a computer, and a data acquisition system (Agilent Co.) as shown in Figure 1. The experimental section includes three parts, *i.e.*, a heating part (100 mm), an energy storage part (100 mm) and a condensing part (100 mm). All the three parts are installed on a flat heat pipe. The flat heat pipe is a copper-water capillary wick structure with

Table 1: Thermophysical properties of PCMs

Parameters	Melting point (°C)	Specific heat (kJ $kg^{-1}°C^{-1}$)	Latent heat (kJ kg^{-1})	Thermal conductivity (W m^{-1} K^{-1})
DI-water	0	4.2	-	0.6
RT30	30±2.5	2.0	163	0.2
RT35	35±2.5	2.0	172	0.2
RT45	45±2.5	1.8	165	0.2

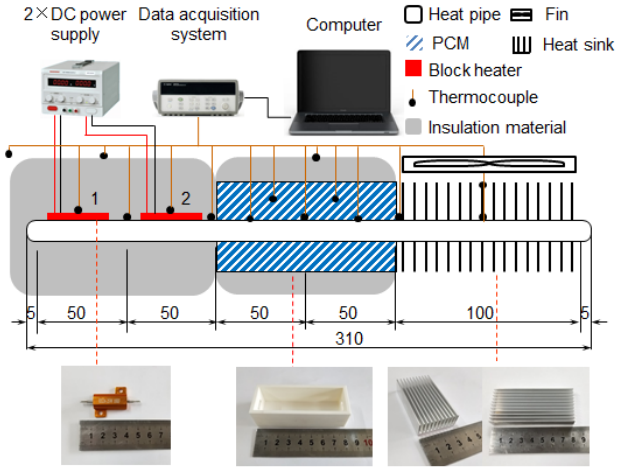

Figure 1: Schematic and photos of experimental setup (unit: mm)

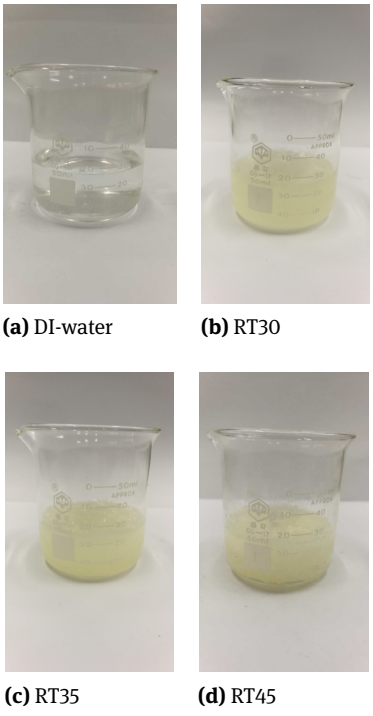

(a) DI-water **(b)** RT30

(c) RT35 **(d)** RT45

Figure 2: Experimental material samples

a length of 310 mm and a width of 11 mm. As shown in Figure 2, several PCMs and DI-water are used as materials for thermal energy storage during the tests. The paraffin was purchased from Nanyang Hannuo Petrochemical Co. Ltd. China. The thermophysical properties of PCMs and DI-water are shown in Table 1.

A heating system with multiple heat sources is installed on the evaporator section of the heat pipe. The heating system consists of two heating modules which generate various heat fluxes by resistors with a direct current. As shown in Figure 1, each heating module has a length of 50 mm and a width of 14 mm. Each heating module contains two heating-resistor blocks connected to two DC power supplies. The input power of the heating system is controlled by adjusting the voltage of the DC power supplies. In order to simulate the real system, the testing section is heated continually until the temperature of the heat source reaches the equilibrium state. To judge the equilibrium state, a criteria is given as: when temperature values of heat sources change less than 1°C within 1 min, it is regarded as equilibrium state.

The container for the energy storage is a tank full of the PCMs. This container with dimensions of 106 mm ×31 mm×23 mm was made from polylactide acid by a 3D printer, and it was covered by insulation materials to reduce the heat dissipation. The gap between the heat pipe and the PCM container is filled with thermal silica gel to avoid the leakage of the PCMs. The condensation section consists a fan and a heat sink attached to the other end of the heat pipe. The heat sink made of aluminum has a total cooling area of 0.128 m^2.

Temperature distributions along the heat pipe and on each part of testing sections are measured by T-type thermocouples. Locations of the thermocouples are shown in Figure 1. In order to heat from the same initial condition, the ambient temperature is measured during each test. In order to record temperature values at different testing positions of the heat pipe and PCMs, thermocouples are arranged in the evaporative section, the adiabatic section and the condensing section of the heat pipe. Another five thermocouples are located along the heat pipe.

Table 2: The heating time and cooling time under different heating conditions

Materials	10 W-10 W		10 W-5 W		5 W-10 W		5 W-5 W	
	Heating time (s)	Cooling time (s)	Heating time (s)	Cooling time (s)	Heating time (s)	Cooling time (s)	Heating time (s)	Cooling time (s)
W/O PCM	1570	1140	770	920	800	1100	680	1020
DI-water	2040	2330	940	2080	950	2280	800	2040
RT30	1640	3940	690	1970	590	1780	610	1540
RT35	1310	4080	780	2070	720	1850	620	1800
RT45	1790	2540	720	1780	680	1290	630	1520

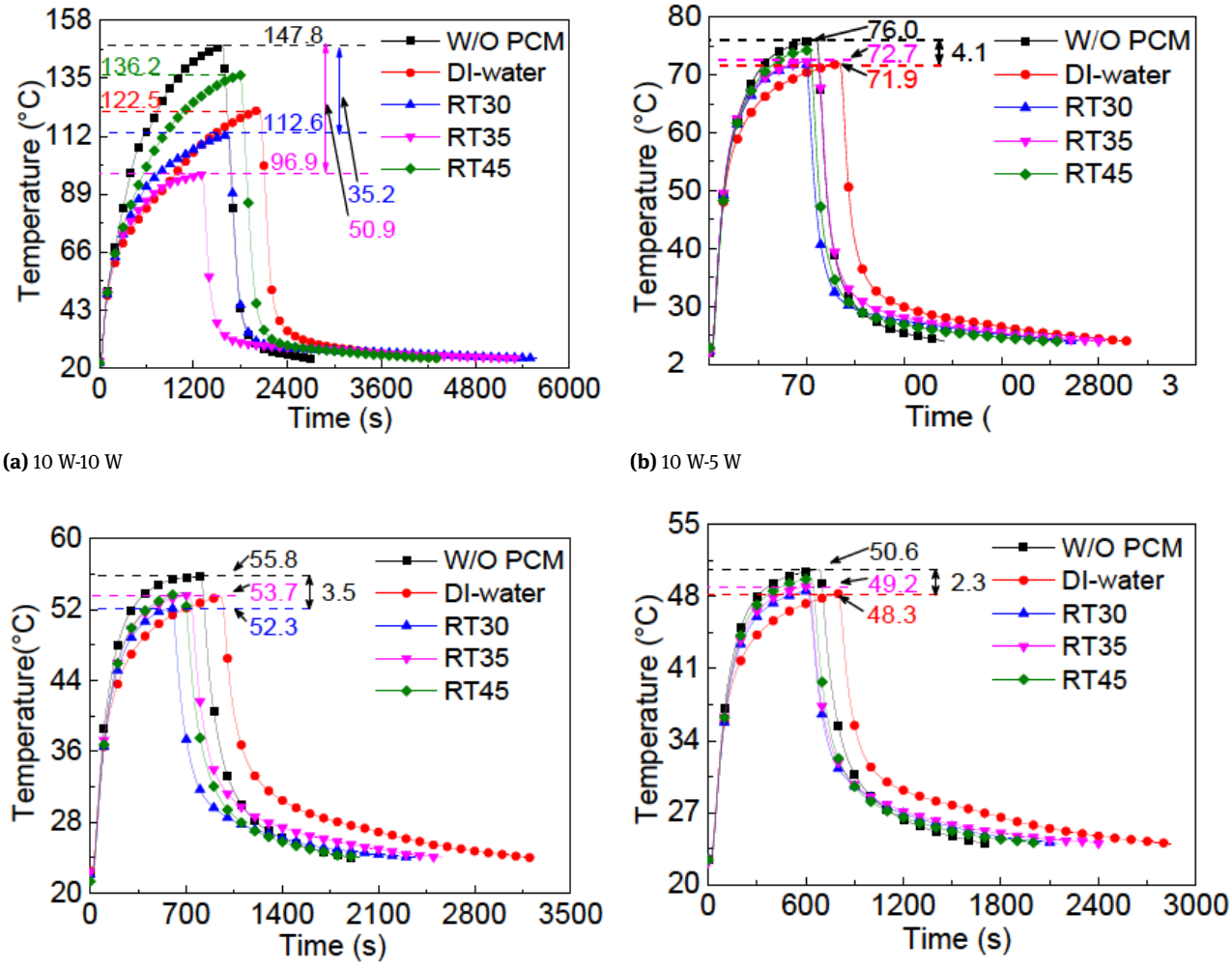

(a) 10 W-10 W

(b) 10 W-5 W

(c) 5 W-10 W

(d) 5 W-5 W

Figure 3: Temperature variations of heat source 1 under different heating conditions (Heat source 1 power–heat source 2 power)

2.2 Uncertainty analysis

The uncertainties of the experimental results are estimated based on an error analysis of the present measurements. T-type thermocouples are calibrated with an accuracy of ±0.2°C, while the data acquisition unit has an accuracy of 0.05°C. Moreover, the input power is supplied by a DC power supply with 0.1% voltage accuracy and 0.5% current accuracy.

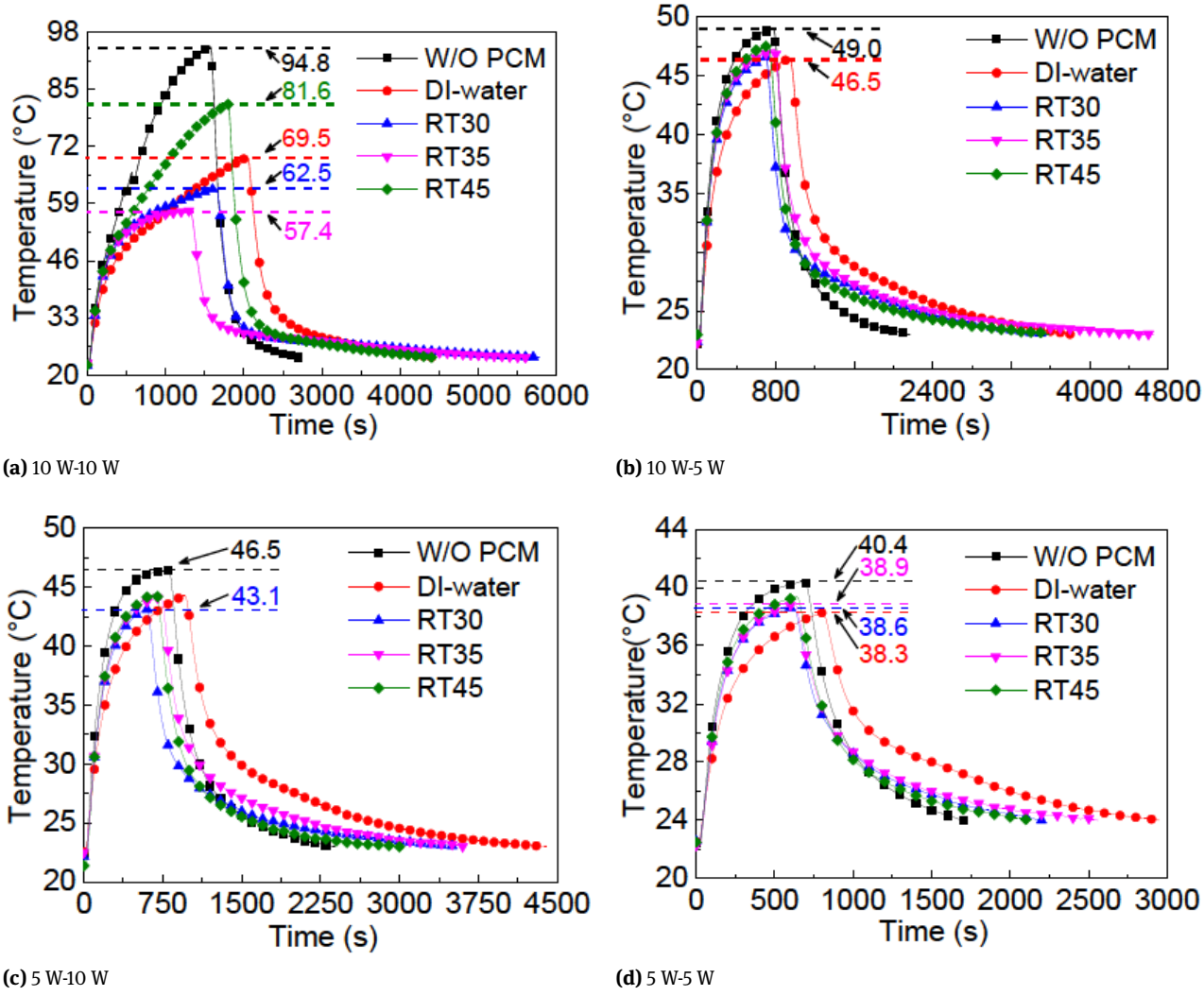

(a) 10 W-10 W **(b)** 10 W-5 W

(c) 5 W-10 W **(d)** 5 W-5 W

Figure 4: Temperature variations of the evaporation section under different heating conditions (Heat source 1 power–heat source 2 power)

3 Results and discussion

In order to investigate the effect of the PCMs on the heat dissipation performance, constant systems with multiple heat sources are used by a variety of power combinations.

3.1 Constant multiple heat sources

In this part, four conditions with constant heat sources are analyzed by using different PCMs. The heat sources 1 and 2 are set to powers of 5 W and 10 W, respectively. Investigations of temperature values on heat sources, evaporation section, adiabatic section, and energy storage part are conducted under both charge and discharge processes of the different heat sources.

Figure 3 shows transient temperature responses during different heat inputs for various PCMs. It is found from Figure 3(a), that temperature value of heat source 1 reaches to 96.9°C for the material RT35 under a heat source of 10 W-10 W. Compared to the case without PCMs (W/O PCM), the temperature of the heat source 1 is reduced by 34.4% (50.9°C) from 147.8°C. Compared with other PCMs, the RT30 also shows a slight advantage for heat dissipation. Moreover, the temperature value of the heat source 1 for the RT30 is 112.6°C, which is 23.8% (35.2°C) lower than that for no PCM material. Although the RT45 can reduce the temperature by 11.4°C compared with no PCMs, the RT45 shows a worse heat dissipation compared to the DI-water. As shown in Figures 3(b)-3(d), the maximum temperature differences between the cases with and without PCM

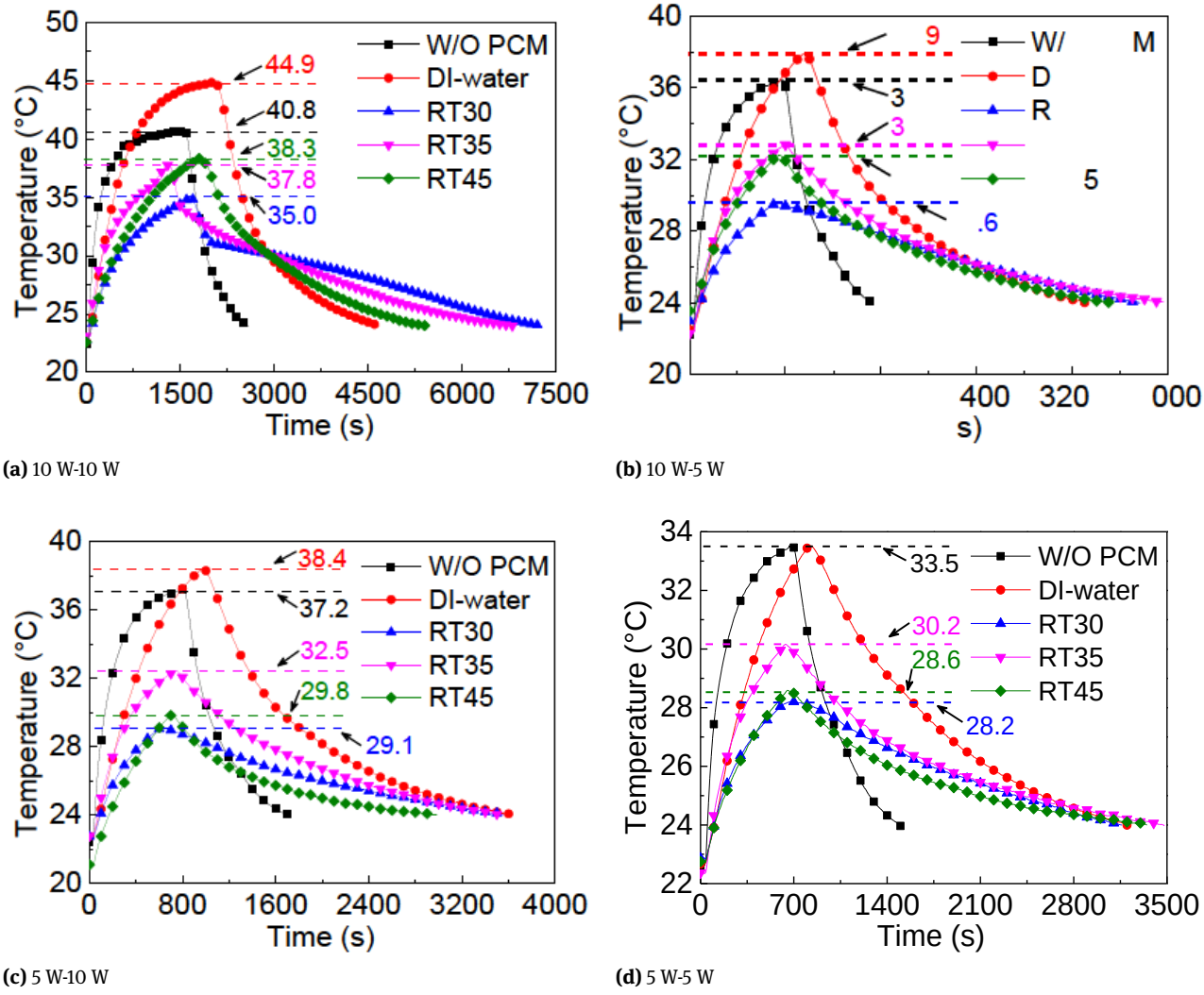

(a) 10 W-10 W

(b) 10 W-5 W

(c) 5 W-10 W

(d) 5 W-5 W

Figure 5: Temperature variations of materials in an energy storage tank under different heating conditions (heat source 1 power–heat source 2 power)

are 4.1°C, 3.5°C and 2.3°C for heating powers of 10 W-5 W, 5 W-10 W, and 5 W-5 W, respectively.

In addition, the equilibrium temperature of the heat source is quickly reached by using the RT35, and the heating stabilization time is 1310 s, as shown in Table 2. The heating stabilization times required for no material, DI-water, RT30 and RT45 are 1570 s, 2040 s, 1640 s and 1790 s, respectively. When the power of the heat source 2 decreases as shown in Figure 3(b), the temperature values for the RT30, RT35 and RT45 show a similar increasing trend. Compared with the data for the cases with no PCMs, DI-water, RT30, RT35 and RT45 in Figure 3(a), the maximum temperature values of the heat source 1 decrease by 71.8°C, 50.6°C, 40.4°C, 24.3°C and 62.1°C, respectively. It is concluded that when the power is relatively high (10 W-10 W), the RT35 shows a better cooling performance due to a high energy storage in the PCM box. However, the results indicate that due to its sensible heat absorption, the DI-water under a low heating power provides a lower heating equilibrium temperature than the PCMs.

Figure 4 presents transient temperature variations of the evaporation section under different heating conditions. Compared with no PCMs, DI-water, RT30 and RT45 as shown in Figure 4(a), the maximum temperature values of the evaporation section for the RT35 are reduced by 39.4%, 17.3%, 8.1% and 29.7%, respectively. Based on a comparison of the results in Figure 4(a) - 4(d), it is found that the RT35 has a higher capacity of energy storage under a high heating power compared with the other materials. When the heat source power changes from 5 W-5 W to 10 W-10 W, the temperature of the evaporation section for the RT35 increases by 47.6% (from 38.9°C to 57.4°C). For the DI-water

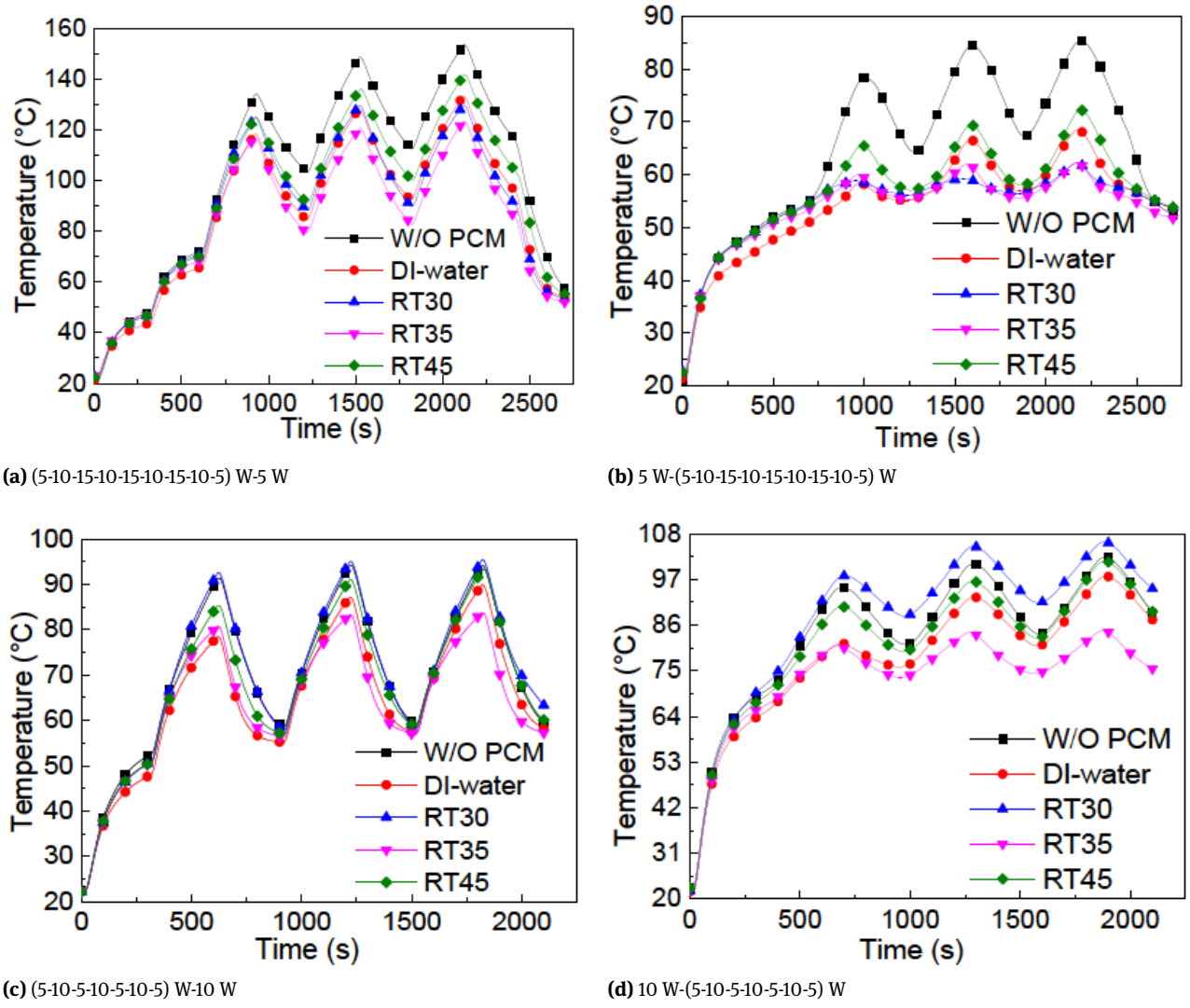

(a) (5-10-15-10-15-10-15-10-5) W-5 W

(b) 5 W-(5-10-15-10-15-10-15-10-5) W

(c) (5-10-5-10-5-10-5) W-10 W

(d) 10 W-(5-10-5-10-5-10-5) W

Figure 6: Temperature variations of heat source 1 under dynamic heating powers (heat source 1 power–heat source 2 power)

and the RT30, the temperature of the evaporation section increases by 81.5% and 61.9%, respectively. However, three PCMs (RT30, RT35, and RT45) under a low heating power show worse cooling performance than the DI-water. It is also concluded that PCMs can provide good cooling protection in a multiple heat source system, which avoids damage of the equipment caused by transient high power operation in a short time.

In charge and discharge processes of heat sources, the temperature variations of materials in the energy storage tank are illustrated by changing the heating conditions as shown in Figure 5. In Figure 5(a), the maximum temperature of the DI-water in the storage tank reaches 44.9°C, and the corresponding equilibrium time is up to 2050 s. When the heat source temperature reaches equilibrium, the temperature values for the RT30 and RT35 are 37.8°C and 35.0°C, respectively. As shown in Figure 5(b), the temperature of the DI-water rises to 37.9°C after 960 s when the heat source temperature reaches equilibrium, whereas the temperature values of the RT30 and RT35 increase to 29.6°C and 32.8°C, respectively. For the heat source in Figure 5(c), the RT30 and RT35 have equilibrium temperature values of 29.1°C and 32.5°C, respectively.

As can be seen from Figure 5(b) and 5(c), the temperatures of the DI-water, RT30 and RT35 in the container are close for the same conditions of the total heat source. With increasing the power as shown in Figures 5(a)-5(b), the temperature values of the DI-water, the RT30 and the RT35 increase by 7.0°C, 5.4°C and 5.0°C, respectively. Decreasing the heating power as shown in Figure 5(d), the equilibrium temperature of the heat source attains lower values

Table 3: The periodical heating processes for dynamic multiple heat sources

Time (min)	Heating condition 1		Heating condition 2		Heating condition 3		Heating condition 4	
	Heat source 1 (W)	Heat source 2 (W)	Heat source 1 (W)	Heat source 2 (W)	Heat source 1 (W)	Heat source 2 (W)	Heat source 1 (W)	Heat source 2 (W)
0-5	5	5	5	5	5	10	10	5
5-10	10	5	5	10	10	10	10	10
10-15	15	5	5	15	5	10	10	5
15-20	10	5	5	10	10	10	10	10
20-25	15	5	5	15	5	10	10	5
25-30	10	5	5	10	10	10	10	10
30-35	15	5	5	15	5	10	10	5
35-40	10	5	5	10	-	-	-	-
40-45	5	5	5	5	-	-	-	-

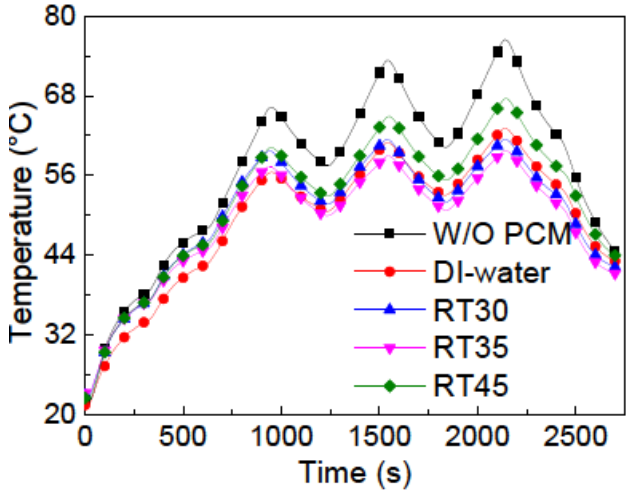

(a) (5-10-15-10-15-10-15-10-5) W-5 W

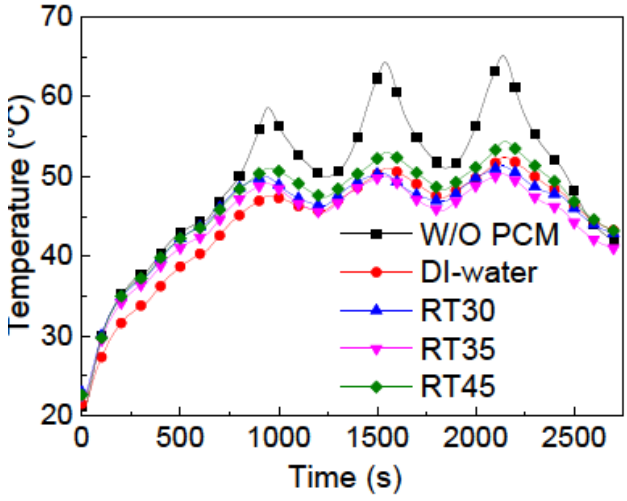

(b) 5 W-(5-10-15-10-15-10-15-10-5) W

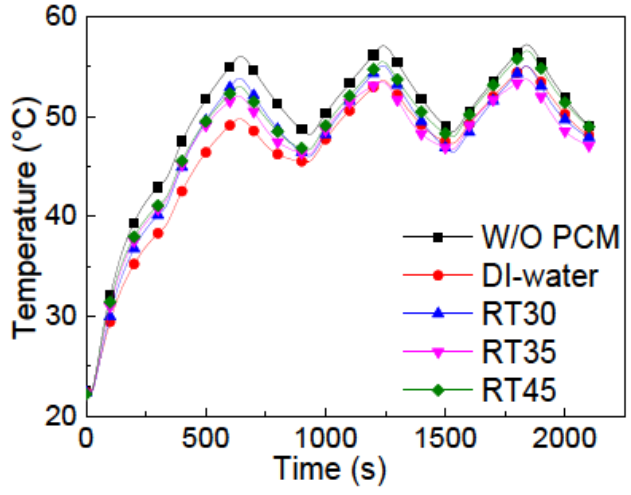

(c) (5-10-5-10-5-10-5) W-10 W

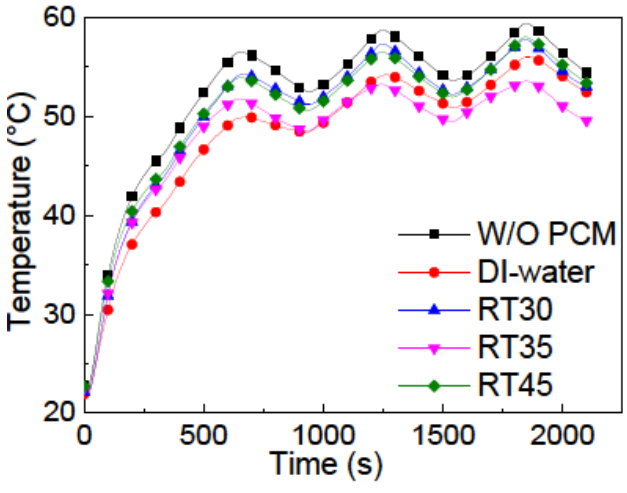

(d) 10 W-(5-10-5-10-5-10-5) W

Figure 7: Temperature variations of the evaporation section under different heating powers (heat source 1 power–heat source 2 power)

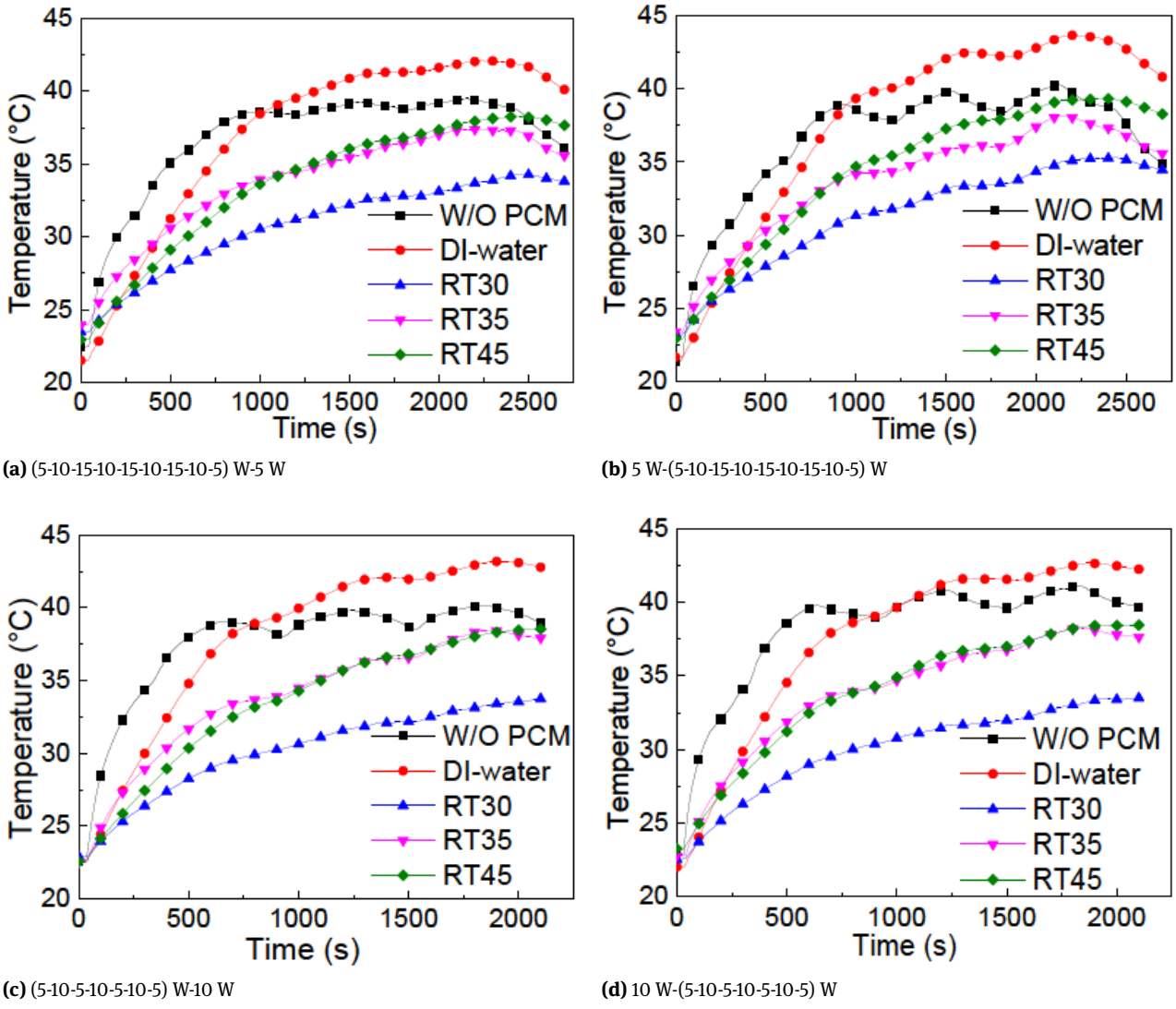

(a) (5-10-15-10-15-10-15-10-5) W-5 W

(b) 5 W-(5-10-15-10-15-10-15-10-5) W

(c) (5-10-5-10-5-10-5) W-10 W

(d) 10 W-(5-10-5-10-5-10-5) W

Figure 8: Temperature variations of materials in an energy storage tank under different heating conditions (heat source 1 power–heat source 2 power)

(33.5°C, 28.2°C, and 30.2°C for DI-water, RT30, and RT35, respectively).

It can be seen from Figure 5(a) that the PCMs in the storage tank are in equilibrium for the DI-water. However, the heating temperature for the DI-water is relatively high, and the heat from the source 1 cannot be effectively dissipated. Although temperature curves for the three PCMs (RT30, RT35, and RT45) have upward trends (that means the PCMs have not reached the equilibrium temperature), the rising temperature values are lower than for the DI-water and no material. This result indicates that PCMs plays an important role in heat dissipation and absorption of heat generation from a multiple heat source system with a high power.

3.2 Dynamic multiple heat sources

In order to analyze heat dissipation performance of various PCMs, Figure 6 shows the transient temperature response of the heat source 1 to dynamic systems with multiple heat sources. One of the two heat sources is kept a fixed power value (5 W or 10 W), and the other heat source varies in dynamic power values (5-10-15-10-15-10-15-10-5 W or 5-10-5-10-5-10-5 W). For dynamic characteristics of the heat pipe with various PCMs, dynamic power changes with an interval of 5 min are considered, as shown in Table 3. It is observed that before a heating time of 750 s, a lower temperature of the heat source 1 is obtained by using the DI-water compared with the PCMs. After a heating time of 1000 s, the material RT35 shows a significant cooling

performance on the heat source 1 as shown in Figure 6(a). Compared with the condition without PCM material during periodic heating, the maximum temperature for the RT35 in the three heating processes is reduced by 12.9%, 18.9% and 19.5%, respectively. For periodic heating with low powers as shown in Figure 6(b), the RT35 shows a larger enhancement of the heat dissipation for the heat source 1 than the other PCMs. Compared with no PCMs, the maximum temperature values in the three heating processes are reduced by 11.6%, 11.6% and 11.0%, respectively.

During the three heating processes, the maximum temperature of the heat source 1 for the DI-water gradually increased from 118.3°C (in the first heating) to 133.2°C (in the third heating). For the RT30, the maximum temperature increases from 124.9°C (in the first heating) to 129.7°C (in the third heating). For the RT35 condition, the maximum temperature of the heat source 1 increases from 116.7°C (in the first heating) to 123.5°C (in the third heating). It is also concluded that the RT35 has more energy storage after a periodic heating, which results in good cooling performance from the RT35 for a dynamic heating power. Compared with the DI-water in the three heating processes, the maximum temperature of heat source 1 for RT35 is reduced by 1.1%, 9.5%, and 13.4%, respectively.

Figure 7 illustrates temperature variations of the evaporation section with time under different heating conditions. It is found that the temperature trends are consistent in Figure 6-7. Temperature values of the evaporation section for the DI-water are lower than for other PCMs in the range of 0-1000 s, whereas temperature values of the evaporation section for RT35 is lowest after 1200 s. According to these results, this study proves that the RT35 effectively provides a lower temperature rise and also more uniform temperature evolutions when a dynamic heating power is given to the evaporation section of the heat pipe. After two periodic heating processes, the temperature of the evaporation section for the RT35 maintains a relatively low value.

Temperature variations of materials in the energy storage tank are analyzed under different heating conditions as shown in Figure 8. It is observed that the maximum temperature values of RT30 and RT35 are steadily rising until they approach the phase transition values of the PCMs. This is because the PCMs can absorb most of the heat flux continuously before the phase transition point due to its sensible heat, and then the latent heat of PCMs works when the temperature reaches the phase transition point. However, the DI-water absorbs all the heat flux by sensible heat because of no phase transition (above 0°C).

4 Conclusions

In this paper, effects of PCMs on transient temperature of heat source, evaporation section, and energy storage characteristics of PCMs were investigated by using a multiple heat source system. Both constant and dynamic systems with two heat sources are studied under various heat source powers. Experimental tests and analysis of results are conducted by changing energy storage materials in a tank, including DI-water, RT30, RT35 and RT45.

Compared with no PCMs, DI-water, RT30 and RT45 for the constant power of heat sources, the maximum temperature values of the evaporation section for the RT35 show reductions of 39.4%, 17.3%, 8.1% and 29.7%, respectively. Based on temperature testing on the evaporation section, it is proved that the RT35 can take away more heat from the evaporation section of the heat pipe and shorten the time required for reaching the heating balance.

Compared with no cooling material under a dynamic power of heat sources, the maximum temperature values for the RT35 in the three heating processes decrease by 12.9%, 18.9% and 19.5%, respectively. It is found that the RT35 under a high power of 20 W (10 W-10 W) can provide a better cooling performance than other PCMs and DI-water, although the DI-water shows a lower heating equilibrium temperature than other PCMs under low heating power ($P \leq 15$ W).

Acknowledgement: This work is supported by the National Natural Science Foundation of China [Grant numbers 51576059 and 51806057] and Project of Innovation Ability Training for Postgraduate Students of Education Department of Hebei Province [Grant number CXZZSS2019012].

References

[1] Ling Z., Zhang Z., Shi G., Fang X., Wang L., Gao X., *et al.*, Review on thermal management systems using phase change materials for electronic components, Li-ion batteries and photovoltaic modules, Renew. Sustain. Energy Rev., 2014, 31, 427–438.

[2] Kandasamy R., Wang X., Mujumdar A.S., Transient cooling of electronics using phase change material (PCM) -based heat sinks, Appl. Therm. Eng., 2008, 28, 1047–1057.

[3] Al-Jethelah M., Al-Sammarraie A., Tasnim S., Mahmud S., Dutta A., Effect of convection heat transfer on thermal energy storage unit, Open Phys., 2018, 16, 861-867.

[4] Ebadi S., Al-Jethelah M., Tasnim S. H., Mahmud S., An investigation of the melting process of RT-35 filled circular thermal energy storage system, Open Phys., 2018, 16, 574-580.

[5] Zhao D., Tan G., Experimental evaluation of a prototype thermoelectric system integrated with PCM for space cooling, Energy, 2014, 68, 658–666.
[6] Emam M., Ookawara S., Ahmed M., Thermal management of electronic devices and concentrator photovoltaic systems using phase change material heat sinks: Experimental investigations, Renew. Energy, 2019, 141, 322–339.
[7] Kalbasi R., Afrand M., Alsarraf J., Tran M., Studies on optimum fins number in PCM-based heat sinks, Energy, 2019, 171, 1088–1099.
[8] Mashaei P.R., Shahryari M., Fazeli H., Hosseinalipour S.M., Numerical simulation of nanofluid application in a horizontal mesh heat pipe with multiple heat sources: A smart fluid for high efficiency thermal system, Appl. Therm. Eng., 2016, 100, 1016–1030.
[9] Sevinchan E., Dincer I., Lang H., A review on thermal management methods for robots, Appl. Therm. Eng., 2018, 140, 799–813.
[10] Tan F.L., Tso C.P., Cooling of mobile electronic devices using phase change materials, Appl. Therm. Eng., 2004, 24, 159–169.
[11] Wang Y., Yang Y., Three-dimensional transient cooling simulations of a portable electronic device using PCM (phase change materials) in multi-fin heat sink, Energy, 2011, 36, 5214–5224.
[12] Wang C., Lin T., Li N., Zheng H., Heat transfer enhancement of phase change composite material: Copper foam/paraffin, Renew. Energy, 2016,96, 960–965.
[13] Ebrahimi A., Hosseini M.J., Ranjbar A.A., Rahimi M., Bahrampoury R., Melting process investigation of phase change materials in a shell and tube heat exchanger enhanced with heat pipe, Renew. Energy, 2019, 138, 378–394.
[14] Abujas C.R., Jové A., Prieto C., Gallas M., Cabeza L.F., Performance comparison of a group of thermal conductivity enhancement methodology in phase change material for thermal storage application, Renew. Energy, 2016, 97, 434–443.
[15] Wang J., Li G., Zhu H., Luo J., Sundén B., Experimental investigation on convective heat transfer of ferrofluids inside a pipe under various magnet orientations, Int. J. Heat Mass Transf., 2019, 132, 407-419.
[16] Chen Z., Zheng D., Wang J., Chen L., Sundén B., Experimental investigation on heat transfer characteristics of various nanofluids in an indoor electric heater, Renew. Energy, 2020, 147, 1011-1018.
[17] Han X., Wang Y., Liang Q., Investigation of the thermal performance of a novel flat heat pipe sink with multiple heat sources, Int. J. Heat Mass Transfer, 2018,94, 71–76.
[18] Zhang S., Chen J., Sun Y., Li J., Zeng J., Yuan W., *et al.*, Experimental study on the thermal performance of a novel ultra-thin aluminum flat heat pipe, Renew. Energy, 2019, 135, 1133–1143.
[19] Chougule S.S., Sahu S.K., Thermal Performance of Nanofluid Charged Heat Pipe With Phase Change Material for Electronics Cooling, ASME J. Electron. Packag, 2016, 137, 1–7.
[20] Shabgard H., Faghri A., Performance characteristics of cylindrical heat pipes with multiple heat sources, Appl. Therm. Eng., 2011, 31, 3410–3419.
[21] Tang H., Tang Y., Li J., Sun Y., Liang G., Peng R., Experimental investigation of the thermal performance of heat pipe with multi-heat source and double-end cooling, Appl. Therm. Eng., 2018, 131, 159–166.
[22] Weng Y.C., Cho H.P., Chang C.C., Chen S.L., Heat pipe with PCM for electronic cooling, Appl. Energy, 2011, 88, 1825–1833.
[23] Zhuang B., Deng W., Tang Y., Ding X., Chen K., Zhong G., Experimental investigation on a novel composite heat pipe with phase change materials coated on the adiabatic section, Int. Commun. Heat Mass Transf., 2019, 100, 42–50.
[24] Behi H., Ghanbarpour M., Behi M., Investigation of PCM-assisted heat pipe for electronic cooling, Appl. Therm. Eng., 2017, 127, 1132–1142.